



Provided by the author(s) and University of Galway in accordance with publisher policies. Please cite the published version when available.

Title	Repeated load testing of two schist and limestone aggregate materials used in unbound forest roads
Author(s)	Rodgers, M., Keaney, J., Healy, M.G.
Publication Date	2009
Item record	<a href="http://hdl.handle.net/10379/2922">http://hdl.handle.net/10379/2922</a>
DOI	<a href="http://dx.doi.org/DOI 10.1016/j.jterra.2009.05.001">http://dx.doi.org/DOI 10.1016/j.jterra.2009.05.001</a>

Downloaded 2024-05-18T13:47:52Z

Some rights reserved. For more information, please see the item record link above.



*Published as: Rodgers, M., Keaney, J., Healy, M.G. 2009. Repeated load testing of two schist and limestone aggregate materials used in unbound forest roads. Journal of Terramechanics 46(6): 285-292.*

REPEATED LOAD TESTING OF SCHIST AND LIMESTONE AGGREGATE  
MATERIALS USED IN UNBOUND FOREST ROADS

M. Rodgers<sup>\*</sup>, J. Keaney and M.G. Healy

Department of Civil Engineering, National University of Ireland, Galway, Ireland.

**Abstract**

This study examined the behaviour of two completion aggregates that were placed on a silty sandy formation material and subjected to repeated loading in a large-scale testing rig. The completion aggregates were (i) a good quality limestone, and (ii) a poor quality schist, and are used in the construction of unbound forest roads in Ireland. The schist was tested on its own and in combination with the completion limestone aggregate for up to 150,000 load applications with a maximum loading pressure of 1000 kPa. Measurements of surface deflections and formation pressures were made during each test. A combination of a 200 mm layer of the limestone aggregate placed on top of a 250 mm layer of the schist aggregate produced the lowest permanent deformations, resilient deflections, and resilient pressures under dry and wet undrained conditions.

---

<sup>\*</sup> Corresponding author. E-mail: [michael.rodgers@nuigalway.ie](mailto:michael.rodgers@nuigalway.ie); Tel: +353 (0)91 492219; Fax: +353 (0)91 494507.

*Keywords:* unbound forest road; repeated loading; formation layer; completion layer; schist and limestone aggregates.

## **Introduction**

In the harvesting of timber from forests, it is necessary to construct unbound roads to carry large, articulated trucks. Forest roads must be built at low cost compared to public roads, and must be maintained cheaply because of the relatively low value of the timber harvested and the long intervals between periods of productive use of the roads.

The pavement layers in unbound forest roads are normally defined as follows:

- (1) A formation layer, which is the underlying *in situ* layer for the road, also known as the subgrade, and
- (2) A completion layer, which is the top layer of the road.

A well-shaped, well-compacted formation provides a firm base for the more costly completion material and should support a solid, maintainable road. During subsequent maintenance, road completion material can always be replaced but a poor formation is effectively impossible to repair [1].

The choice of completion material is critical for the trafficability of the unbound road. For low-cost roads, economics often dictate that, instead of importing suitable road materials, less preferable local materials are used as completion materials. Unbound roads with a high proportion of unsuitable fine-grained completion material may be subject to surface disintegration due to its low shear strength [2, 3]. As the contact pressure from a tyre is mainly supported by the completion layer, the load from the tyre can increase the pore water pressure in the road material when drainage is restricted. This pore water pressure increase can make unsuitable completion material unstable and may result in permanent deformation of the road surface [2]. If the local aggregate is of poor quality, it may be necessary to avoid its use, or else use it under a reduced layer of imported high quality material, thus effecting some cost savings.

Failure of an unbound road structure occurs when surface deformations become unacceptable for traffic [4]. Progressive deterioration of the formation may result from the decrease of its shear strength, possibly due to a progressive increase in pore water pressure if the material is undrained, or to fatigue generated by repeated loading. This deterioration results in [4]:

- (1) acceleration of the occurrence of unacceptable surface deformations resulting from the accumulation of small permanent deformations;
- (2) decreased shear strength of both the formation and completion materials, and
- (3) decreased mechanical ability of the completion material to distribute loads because of thickness reduction, resulting in unacceptable applied stresses to the formation material.

As a result, ruts can develop at the surface of the completion layer over time. The rut depth,  $s$  (mm), may be calculated for geosynthetic, reinforced pavements from [5]:

$$s = \frac{\frac{P}{\pi r^2} f_s}{\left[ \frac{h + 0.204h(R_E - 1)}{0.868r + r(0.661 - 1.006J^2) \left(\frac{r}{h}\right)^{1.5} \log N} + 1 \right]^2 \left[ \left[ 1 - 0.9 \exp\left[-\left(\frac{r}{h}\right)^2\right] \right] N_c c_u \right]} \quad (1)$$

where  $J$  ( $\text{m N}^0$ ) is the aperture stability modulus of the geogrid;  $r$ , the radius (m) of the equivalent tyre contact area;  $h$ , the thickness (m) of the completion layer;  $N$ , the number of loading cycles;  $P$  (kN), the wheel load;  $N_c$ , the bearing capacity factor;  $f_s$ , the maximum allowable rut depth (75 mm); and  $c_u$  (kPa), the undrained cohesion of the formation layer. The limited modulus ratio,  $R_E$ , can be calculated from [5]:

$$R_E = \min\left(\frac{E_{cl}}{E_{fl}}, 5.0\right) = \min\left(\frac{3.48\text{CBR}_{cl}^{0.3}}{\text{CBR}_{fl}}, 5.0\right) \quad (2)$$

where  $E_{cl}$  and  $E_{fl}$  are the completion and formation layer resilient moduli (kPa), respectively, and  $\text{CBR}_{cl}$  and  $\text{CBR}_{fl}$  are the California Bearing Ratios (%) of the completion layer and formation layer aggregates, respectively.

This study was carried out to establish the suitability of a schist aggregate in unbound forest road construction as a completion-layer material on its own, and in combination with a completion limestone aggregate. The tested aggregates are used by the Irish forestry company, Coillte Teoranta. The study objectives were:

- (1) to design and build a repeated load testing machine to test completion materials used in unbound forest road construction, and
- (2) to classify limestone and schist aggregate completion materials and perform repeated load tests on the materials under dry and wet undrained conditions.

## **Materials and Methods**

### *Aggregate testing*

The formation material was a silty, sandy soil from Castledaly Forest - a Coillte Teoranta plantation located approximately 40 km south-east of Galway City. The two completion materials were: a limestone aggregate from Galway and a schist aggregate from Ardara, Co. Donegal. The Galway limestone met the Department of Environment (D.O.E.) Clause 810 specification for wet-mix macadam (WMM) and is commonly used as a road base material in Ireland. The Donegal metamorphic schist contained quartz, which is a strong mineral that can contribute to the durability of an aggregate.

### *Placement of materials and instrumentation*

The aggregates were compacted in a bin, 1.2 m x 1.2 m in plan, on top of a 1000 mm-deep formation material (Figure 1), and tested at different thicknesses and combinations. Following assembly, the bin was lined with polythene sheeting to prevent moisture loss from the formation material. This smooth sheeting also reduced the friction between the formation and completion materials, and the walls of the bin. The formation material and the completion materials were placed in the bin close to their optimum water contents (OWCs). The soil was compacted in 50-mm layers using a KANGO vibrating hammer. During the compaction of the soil, water contents were continuously taken while nuclear probe readings and two sand replacement tests were carried out to monitor the compaction of the soil.

Linear strain conversion transducers (lscts) (MPE Transducers Ltd., UK), with an excitation voltage of 10 volts d.c. and an output range of 0-200 millivolts d.c., recorded the resilient and permanent surface deformation taking place in the aggregate layer. Dial gauges were also used to measure surface deformations. Four 100 mm-diameter oil-filled pressure cells with transducers (Soil Instruments Ltd., England) were placed at heights of 300 mm, 500 mm, 700 mm and 900 mm above the bin base as the soil was compacted, and were used to measure the stresses within the silty sand formation layer. Large-range pressure cells (0-10 bar) were placed towards the top of the bins (C and D in Figure 1) and smaller range cells (0-2 bar) were placed near the bottom (A and B in Figure 1). The pressure cell transducers operated on a 0 - 100 mV output for an excitation voltage of 10 volts d.c.

LabVIEW (National Instruments Ltd., Austin, USA) software application package was used in conjunction with an analogue to digital card to record the responses of all the transducers on a PC. Prior to any testing, the Iscts were calibrated using a micrometer screw and the pressure cell transducers were calibrated in a water-filled triaxial cell.

### *Loading rig construction*

A repeated-load testing rig was designed and constructed to apply pressures, similar to that of a truck tyre, to the aggregate materials (Figure 1). The rig frame comprised four columns and two beams, all of which were manufactured from a 305 x 165 UB 40 size section. End plates were welded to the beams and base plates to the columns using a 6 mm continuous fillet weld. The beams, on which the repeated load actuator was mounted, were connected to the columns using M20 Grade 8.8 bolts and a suitably designed pattern of holes was drilled in the columns to facilitate adjustment of the height of the beams. The columns were braced to the laboratory wall with angle iron to provide stability. Four 200 mm x 25 mm plates were butt-welded to adjoining columns, towards the top and the bottom of the columns, and an angle iron was bolted across the beams at two different locations to provide additional stability. Two 700 mm x 700 mm x 200 mm-deep foundations were constructed in the existing concrete floor. In each foundation, four horizontal T16 steel bars, 800 mm long, were used for reinforcement. To allow for connection of the base plates, 8 M20 Grade 8.8 x 180 mm-long bolts were countersunk to a depth of 140 mm in each foundation pad. C40 concrete was used in the foundations.



The loading pad comprised a 200 mm diameter x 45 mm-thick rubber block (Dunlop, England) attached to the end of the piston on the hydraulic actuator through a universal joint assembly. This universal joint allowed for uniform contact between the completion layer and the pad during testing. In this study, vertical pressures were applied to the unbound surface layer, and resulted in a combination of vertical, horizontal and shear stresses in the completion and formation layer materials. Similar loading techniques have been used in other studies [6].

#### *Classification tests and loading regime*

Classification tests were carried out on both the formation and completion materials in accordance with BS 1377 - Method of test for soils for civil engineering purposes [7]. These tests included natural water content, Atterberg limits, specific gravity and particle size distribution.

The completion materials were also tested for durability - a measure of an aggregate's resistance to environmental influences like wetting, thermal expansion/contraction and freeze/thaw effects. Durability was tested using the magnesium sulphate soundness value (MSSV) test and the water absorption value (WAV) test. An MSSV > 75 % is required for all road base and sub-base aggregates and a WAV < 2 % is required for most road aggregates. The completion layer aggregates were also tested for Aggregate Crushing Value (ACV) [8], 10% Fines Value (TFV) [8], Aggregate Impact Value (AIV) [9], Aggregate Abrasion Value (AAV) [8], and CBR [8].

A total of three tests were carried out: two tests on different layer thicknesses (250 mm and 150 mm) of the schist and one test using a combination of 200 mm of Clause 810 on top of 250 mm of the schist (Table 1). The repeated loading was applied at the rate of one cycle every 3 seconds. Each test lasted 150,000 cycles, providing failure of the material did not occur, and the loading regime was as follows:

50 x 10<sup>3</sup> cycles at an applied pressure of 500 kPa (lightly-loaded axle)  
50 x 10<sup>3</sup> cycles at an applied pressure of 750 kPa (normally-loaded axle)  
50 x 10<sup>3</sup> cycles at an applied pressure of 1000 kPa (heavily-loaded axle)

At the two lower loadings, this regime provided a level of conditioning in the completion material before it was subjected to a subsequent higher applied pressure. After 50 x 10<sup>3</sup> cycles, for Test 2 (Table 1) on the 150 mm schist and for Test 3 (Table 1) on the 2-layered completion combination of limestone and schist, a volume of water equivalent to 10 mm of rainfall was sprayed onto the completion material surface. The water was allowed to soak into the aggregates for 1 hour. The repeated loading test was restarted at an applied pressure of 500 kPa and a comparison was made between the deflection and pressure performances in the dry state and in the wet undrained state. There is evidence in the literature to suggest that the stress history affects the permanent deformation of a granular medium [10]. When gradual loads are applied, the material is progressively stiffened, and this causes a reduction in the proportion of permanent to resilient strains in subsequent cycles.

The physical responses measured during the repeated load testing were:

- (1) The permanent and resilient deformations of the completion material surface, and
- (2) The resilient formation pressures at the pressure cell locations

#### *Identification of model parameters*

The validity of Eqn. 1 for the prediction of the rut depth,  $s$ , was investigated by comparing the measured versus the estimated values of  $s$ . As the aggregates were unreinforced and unpaved,  $J = 0$  and  $N_c = 3.14$  [5]. The radius of the tyre contact area,  $r$ , was 0.1 m. E-values for the formation and completion layers were used to calculate  $R_E$ . In order to estimate the E values of the formation and completion materials for Eqn. 1, a series of elastic-plastic simulations with various E values were conducted using SIGMA/W (SIGMA/W, GEO-SLOPE International Ltd., Alberta, Canada), and the resilient pressures and deflections from these simulations were compared with those recorded in the repeated loading experiments carried out in the test rig. The formation material cohesion,  $c$ , and soil friction angle,  $\Phi$ , - some of the parameters required for SIGMA/W to model residual responses - were determined from a shear box test, and the Poisson's ratio,  $\nu$ , for the formation material was assumed. The corresponding parameters used to model the schist and limestone were based on published literature.

SIGMA/W contains three separate programs: Define, Solve and Contour. The Define program involves the plotting of the system geometry. The Solve program is used to compute the deformations and stress changes. The Contour program graphs the computed

parameters. SIGMA/W comprises eight elastic and plastic constitutive soil models, all of which may be applied to two-dimensional plane strain and axisymmetric problems. All the materials tested showed signs of plastic behaviour due to their continual increase in permanent deformation with increasing number of loading cycles. The elastic-plastic SIGMA/W model using axisymmetric analyses was therefore used for modelling the experimental results.

## **Results**

### *Soil classification tests*

Properties of the completion and formation materials are given in Table 2 and their particle size distributions in Figure 2. The formation material was a well graded, silty sand of low plasticity. This material exhibited quite high CBR values (15%).

The two completion materials were both well-graded, granular materials. The peak CBR of the schist was 36% while that of the Clause 810 aggregate was 156%. The CBR value of the Clause 810 material was well above the 80% CBR value recommended by Giroud and Noiray [11] to ensure adequate spreading of pressure from an applied load. When tested in a dry state, the ACV and the AIV of the schist compared favourably with those of the Clause 810 aggregate.

Due to the higher WAV, the schist was more susceptible to breakdown in the MSSV test than the Clause 810 material, indicating that it could be more sensitive to the effects of frost action.

### *Laboratory repeated loading tests*

#### *Resilient pressures*

In Test 1 (250 mm layer of schist), a maximum resilient pressure of 110 kPa was measured in Cell D at an applied pressure of 1000 kPa (Figure 3) with a resilient deformation of less than 2 mm (Figure 4) and a permanent deformation of about 10 mm (Figure 5). In Test 2, the schist thickness depth was reduced to 150 mm to establish if this thickness was sufficient to support the applied loading. At an applied pressure of 500 kPa, the maximum resilient pressure at Cell D was 131 kPa – over double that measured for the 250 mm-thickness layer. This cell pressure increased to 169 kPa at an applied pressure of 750 kPa and the test was stopped after a total of 61,500 loading cycles to protect the loading apparatus. In Test 3 (200 mm layer of Clause 810 on top of a 250 mm layer of schist), the lowest Cell D resilient pressures were recorded. Under an applied pressure of 1000 kPa, the maximum Cell D resilient pressure in Test 3 was only 36 kPa.

#### *Resilient deflections*

In Test 1 (250 mm layer of schist), at an applied pressure of 500 kPa, a maximum resilient deflection of 1.2 mm was measured (Figure 4). This increased to maximum values of 1.5 mm and 1.8 mm under applied pressures of 750 kPa and 1000 kPa, respectively. In Test 2, the reduction from 250 mm to 150 mm in the schist layer resulted in a resilient surface deformation of about 2.5 mm in the aggregate at an applied pressure of 750 kPa. Test 3 (200 mm layer of Clause 810 on top of a 250 mm layer of schist) had the lowest resilient deflections of all the tests, with maximum resilient deflections of 1.0 mm at an applied pressure of 1000 kPa.

#### *Permanent deformations*

In Test 1 (250 mm layer of schist), 68% of the permanent deformation occurred within the first 10,000 cycles, with permanent deformation equalling 10.2 mm after 150,000 cycles (Figure 5). When 10 mm simulated rainfall was subsequently applied to the schist, a contact pressure of 500 kPa caused a further 7.2 mm of deformation in 3,500 loading cycles – an amount equal to 70% of the deformation that had occurred over the previous 150,000 loading cycles in dry conditions. In Test 2 (150 mm layer of schist), the permanent deformation reached 20.4 mm under an applied pressure of 500 kPa – over double the permanent deformation measured in Test 1 when the layer thickness was 250 mm. When the applied pressure was increased to 750 kPa in Test 2, the permanent deformation quickly increased to a maximum of 24.3 mm and the test was suspended after a total of 61,500 cycles, to prevent damage to the loading apparatus. In Test 3 (200 mm layer of Clause 810 on top of a 250 mm layer of schist), the test pavement performed

satisfactorily with only 4.0 mm of permanent deformation occurring over 150,000 cycles. The pavement still performed well, following the simulation of 10 mm rainfall, with only an increase of 1 mm of deformation occurring over 9,000 loading cycles at a 500 kPa contact pressure.

#### *Prediction of rut depths under repeated loadings*

The parameters used in SIGMA/W are tabulated in Table 3. The E values for the formation material were estimated from a separate experiment where a pressure of 150 kPa was applied directly to the surface of the formation material. Using the E values of 29 MPa for the top 50 mm of the formation layer and 37 MPa for the soil below the top 50 mm layer in SIGMA/W, the simulated results compared well with the experimental results (Table 4). Using an E value of 150 MPa for the schist and the above E values for the formation soil led to good fits of resilient pressures and deflections for Test 1 with the 250 mm completion layer of schist (Table 4). Further simulations were carried out to model Test 3 with the 200 mm layer of Clause 810 on a 250 mm layer of schist and the results from these simulations also compared closely with the measured values (Table 4).

The resulting E-values obtained by calibrating the finite element model, SIGMA/W, are given in Table 5. These values were used to predict the rut depths or permanent deformations using Eqn. 1 (Table 6). The rut depths at three cycles - 50,000, 100,000 and 150,000 - were examined. In this study, the calculated values of the permanent deformations were, in general, of the same order (within 6 mm) as those measured in the

loading rig, except for the 0.15 m deep schist layer after  $50 \times 10^3$  loading cycles at 500 kPa.

## **Conclusions**

The main observations from the study were:

- (i) At a layer thickness of 150 mm, the Donegal schist was not capable of supporting repeated pressures above 500 kPa under dry conditions.
- (ii) At a layer thickness of 250 mm, the schist was capable of supporting repeated pressures up to 1000 kPa under dry conditions, but performed poorly at repeated pressures of 500 kPa under wet undrained conditions
- (iii) A combination of 200 mm of the Clause 810 limestone aggregate over a 250 mm layer of schist performed well at pressures up to 1000 kPa under dry and wet undrained conditions.
- (iv) There was close agreement between the measured and modelled resilient deformations and pressures
- (v) There was reasonable agreement between the measured and modelled permanent deformations

## **Acknowledgements**



This project was part-funded by the Council for Forest Research and Development (COFORD) under the operational Programme for Agriculture, Road Development and Forestry, supported by EU structural funds. Financial support was also obtained from Coillte Teoranta. The authors would like to express their appreciation to Mr. Tom Ryan, Coillte Teoranta, and the late Dr. John Mulqueen, NUI, Galway.

## References

- [1] Anstey J. Construction: achieving low cost/local resources. Low cost unsurfaced roads. Forestry Engineering Specialist Group, Heriot Watt University, Edinburgh, March 22<sup>nd</sup>, 1993.
- [2] Simonsen E, Isacsson U. Thaw weakening of pavement structures in cold regions. *Cold Regions Science and Technology*: 1999: 29(2): 135 – 151.
- [3] Lekarp F, Isacsson U, Dawson A. State of the art: I: Resilient response of unbound aggregates. *Jnl of Transportation Engineering*: 2000: 126(1): 66 – 75.
- [4] Giroud JP, Ah-Line C, Bonaparte R. Design of unpaved roads and trafficked areas with geogrid. Symposium on polymer grid reinforcement. Institution of Civil Engineers, London, 1984.
- [5] Giroud JP, Han J. Design method for geogrid-reinforced unpaved roads. II. Calibration and applications. *Jnl of Geotechnical and Geoenvironmental Engineering*: 2004: 130(8): 787 – 797.
- [6] Moghaddas Tafreshi SN, Khalaj O. Laboratory tests of small-scale HDPE pipes buried in reinforced sand under repeated load. *Geotextiles and Geomembranes*: 2007: 26(2): 145 – 163.
- [7] BS 1377. Method of test for soils for civil engineering purposes. British Standard Institution, London, 1990.
- [8] BS 812. Methods for sampling and testing mineral aggregates, sands and fillers. British Standard Institution, London, 1990.

[9] BS 812. Methods for sampling and testing mineral aggregates, sands and fillers. British Standard Institution, London, 1975.

[10] Lekarp F, Isacsson U, Dawson A. State of the art. II: Permanent strain response of unbound aggregates. *Jnl of Transportation Engineering*: 2000: 126 (1): 76 – 83.

[11] Giroud JP, Noiray L. Geotextile reinforced unpaved road design. *Jnl of Geotechnical Engineering Division* 1981:107 (9):1233 – 1254

## **List of figures**

Figure 1. Laboratory loading apparatus.

Figure 2. Particle size distributions for the materials.

Figure 3. Resilient pressures, measured 900 mm from the base of the formation layer, versus number of loading cycles.

Figure 4. Maximum resilient deflections, measured at the centre of the completion layer surface, versus number of loading cycles.

Figure 5. Maximum permanent deformations, measured at the centre of the completion layer surface, versus number of loading cycles.

Table 1. List of full-scale tests.

Test no.	Material	Thickness <sup>†</sup> m	Optimum water content %	Initial water content %	Final dry density Mg m <sup>-3</sup>
1	Schist	0.25	6.0	6.3	1.89
2	Schist	0.15	6.0	6.0	1.96
3	0.2 m Clause 810 on top of 0.25 m schist <sup>‡</sup>	0.2 (0.25)	2.5 (6.0)	3.0 (6.3)	2.09 (2.02)

<sup>†</sup> Thickness refers to the completion layer. The formation material had a thickness of 1 m for all tests.

<sup>‡</sup> Schist is denoted by the brackets.

Table 2. Summary of BS laboratory test results.

Laboratory tests	Limits	Formation Castledaly	Completion Clause 810	Schist
Natural moisture content (%)	-	22.0	-	-
Liquid limit (%)	-	33.3	18.3	38.5
Plastic limit (%)	-	22.6	-	-
Plasticity index (%)	0-6	10.7	0	0
Specific gravity (Gs)	-	2.6	2.7	2.8
Max. dry density (Mg m <sup>-3</sup> )	-	1.8	2.3	2.1
Optimum water content (%)	-	13.5	6.1	8.7
California bearing ratio (%) <sup>†</sup>	2/30	15.0	156.0	36.0
Flakiness index (%)	<35.0	-	19.6	31.0
Magnesium sulphate soundness value (%)	>75.0	-	93.8	80.3
Water absorption value (%)	<2.0	-	0.3	1.2
Dry aggregate crushing value (%)	<35.0	-	21.3	19.8
Wet aggregate crushing value (%)	<35.0	-	22.8	30.0
Dry aggregate impact value (%)	<35.0	-	15.2	22.0
Wet aggregate impact value (%)	<35.0	-	16.0	31.6
Aggregate abrasion value (%)	<10.0	-	11.0	11.1
Effective size, d <sub>10</sub> , (mm)		3.8x10 <sup>-3</sup>	9.5x10 <sup>-1</sup>	3.2

<sup>†</sup> The minimum allowable *in situ* CBR for a subgrade soil is 2%.

Table 3. Soil parameters used in SIGMA/W.

---

Material	c (kPa)	$\Phi$	$\nu$
Formation	34.9	36	0.35
Schist	5	40	0.3
Limestone (Cl.810)	5	40	0.3

---

Table 4. Comparison of resilient measured and modelled pressures in the formation material and deflections under the loading pad at different applied pressures.

Test	Material	Thickness (m)	Applied pressure (kPa)		Pressure measured in pressure cells <sup>†</sup> (kPa)				Deflection (mm)
					A	B	C	D	
1	Formation	1	150	Measured	4.5	7	21	68	0.68
				Modelled	4.7	8.5	22	84	0.68
	Schist	0.25	500	Measured	11	13.5	28	60	1.14
				Modelled	9.5	14	27	62	1.14
			750	Measured	17	19.5	40	83	1.50
				Modelled	14.5	22	41	90	1.50
			1000	Measured	23	26	54	106	1.79
				Modelled	20	30	54	114	1.79
3	Clause 810/Schist	0.2/0.25	500	Measured	24	13	8	8	0.56
				Modelled	19	11.5	7.5	5.5	0.41
			750	Measured	29	21	12	12	0.76
				Modelled	31	19	12	9	0.64
			1000	Measured	34	25	16	15	0.70
				Modelled	42	26.5	17	12.5	0.88

<sup>†</sup> Pressure cells A, B, C and D were at respective heights of 300, 500, 700, and 900 mm from the base of the formation material (Fig. 1).



Table 5. Estimation of resilient moduli, E.<sup>†</sup>

Test	Material	Material depths (m)	Applied pressure (kPa)		
			500	750	1000
			_____ Calculated resilient moduli, E (kPa) _____		
	Formation	1	37	37	37
1	Schist	0.25	115	150	190
3	Clause 810 (over 0.25 m schist)	0.2	550	550	550

<sup>†</sup> The resilient moduli for the soils were estimated by calibrating the SIGMA/W finite element model of the soils and loadings to provide resilient modelled deflections under the centre of the loading pad that were in good agreement with the measured experimental results.

Table 6. Comparison of modelled versus measured rut depths.

Test	Material	Thickness m	No. of cycles		rut depth, s			
			0-50,000 at 500 kPa	50,000 – 100,000 kPa at 750kPa	0-50,000 at 500 kPa	50,000 – 100,000 at 750 kPa	100,000 –150,000 at 1000kPa	Calculated mm
1	Schist	0.25	1.5	7.7	3.2	9.0	5.0	10.2
2	Schist	0.15	2.0	20.4	-	-	-	-

Figure 1.

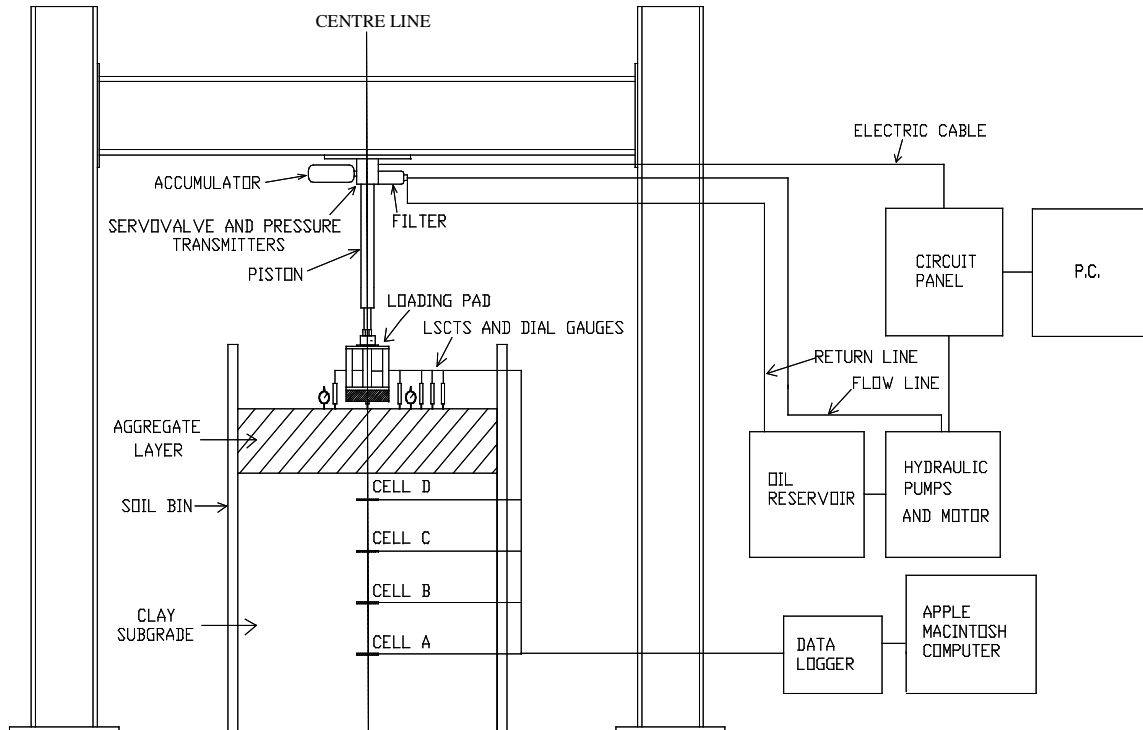


Figure 2.

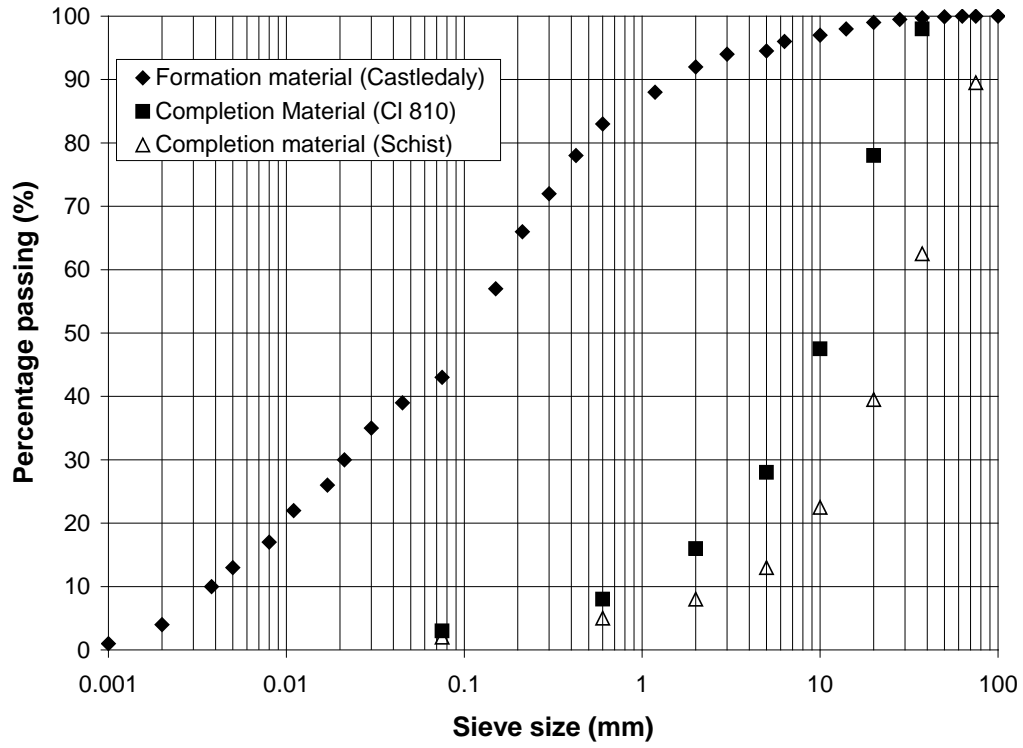


Figure 3.

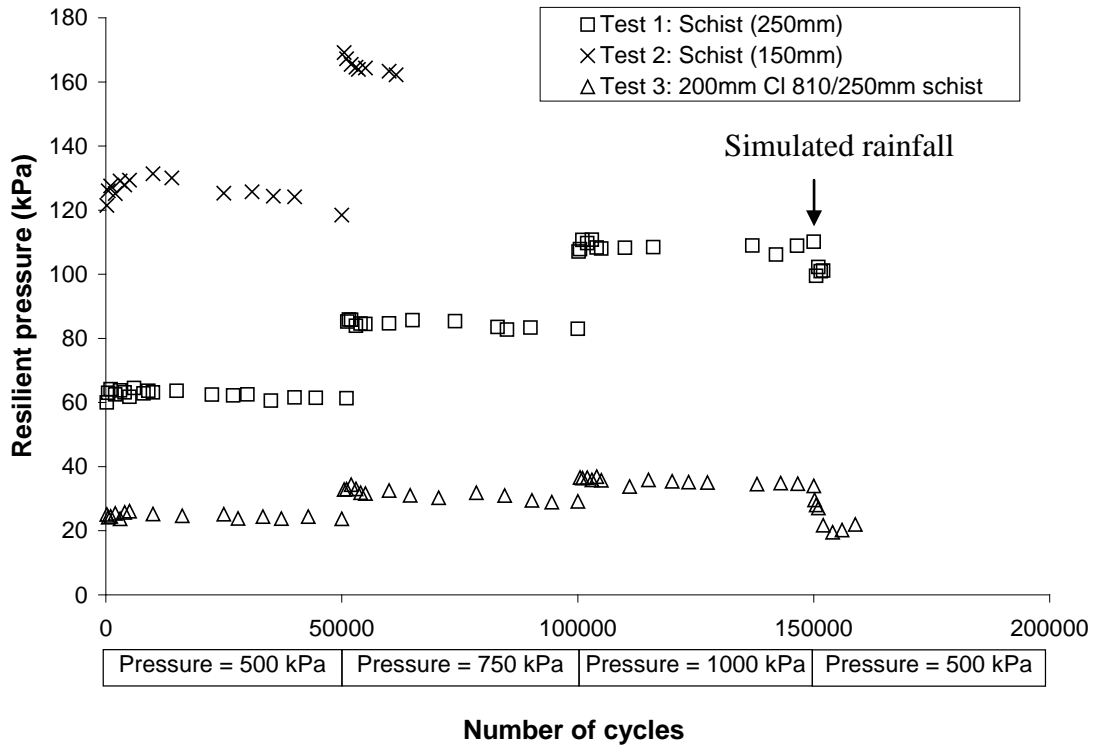


Figure 4.

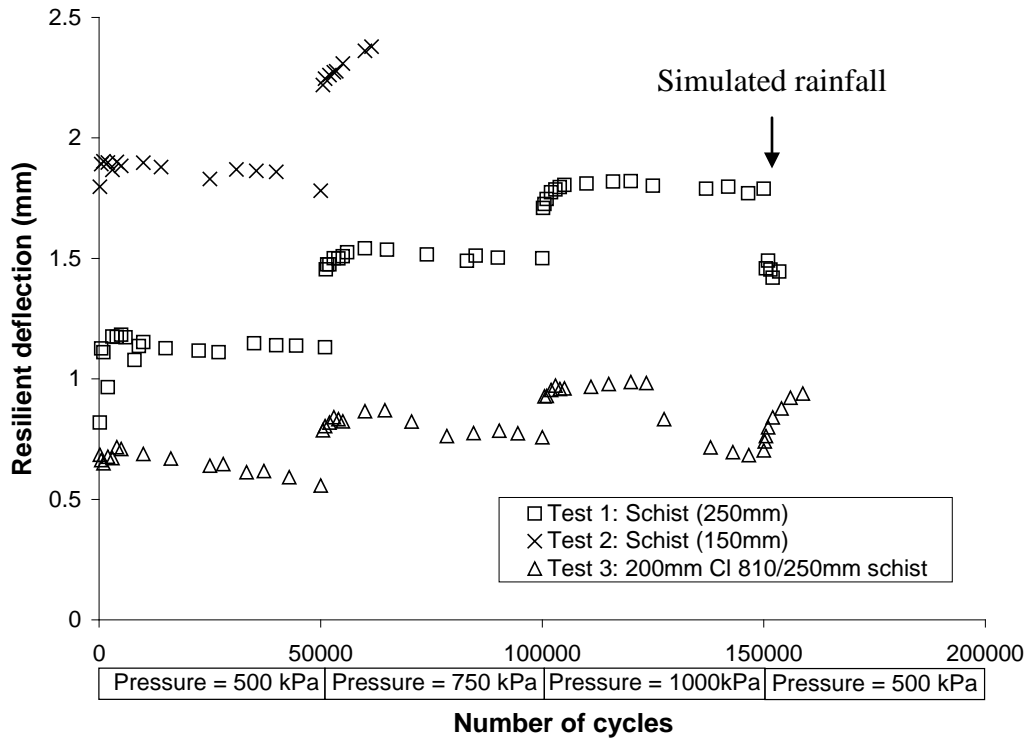


Figure 5.

